Nanoscale

Accepted Manuscript

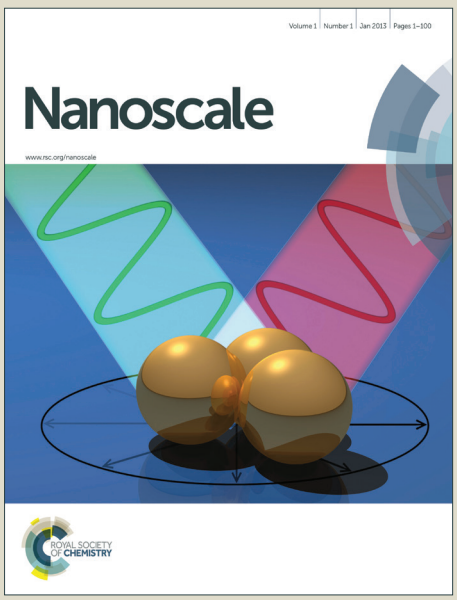

ROYAL SOCIETY OF CHEMISTRY

www.rsc.org/nanoscale

Journal Name

RSCPublishing

COMMUNICATION

An *in situ* Approach ~~to~~ for Facile Fabrication of Robust and Scalable SERS Substrates

Cite this: DOI: 10.1039/x0xx00000x

Yi-Chung Wang,[a] Joseph S. DuChene,[a] Fengwei Huo,[b] and Wei David Wei[a*]

Received 00th January 2012,
Accepted 00th January 2012

DOI: 10.1039/x0xx00000x

www.rsc.org/

The widespread implementation of surface enhanced Raman scattering (SERS) techniques for chemical and biological detection requires an inexpensive, yet robust SERS substrate with high sensitivity and reproducibility. To that end, we present a facile method to fabricate plasmonic SERS substrates with well-distributed SERS "hot spots" on a large scale with reproducible SERS enhancement factors of ~10^8 for the Raman probe molecule 4-aminobenzenethiol (4-ABT). The SERS enhancement is attributed to the synergistic interactions between the strong plasmonic coupling among the assembled Au NPs and the structure-associated tip enhancement. Additionally, these mechanically-flexible substrates exhibit remarkably reproducible SERS signals, demonstrating the merits of our methodology. Our approach illustrates the potential opportunities for fabricating robust, commercially-viable SERS substrates with well-distributed "hot spots" on a large scale while avoiding costly vacuum deposition technologies.

Introduction

Surface enhanced Raman scattering (SERS) has recently garnered extensive scientific interest due to the growing demand for reliable, miniaturized devices that boast low detection-limits for molecular diagnostics.[1-6] In SERS, the excitation of the localized surface plasmon resonance (LSPR) of noble metal (i.e. Au, Ag, Cu) nanostructures generates an enhanced electromagnetic (EM) field that significantly amplifies the optical cross-section of Raman molecules adsorbed on the nanostructure surface.[7-13] It has been reported that nanostructures with SERS enhancement factors (EFs) higher than 10^8 orders of magnitude are capable of detecting single molecules.[2, 14, 15] However, such nanostructures are typically made of Ag and commonly constructed from ordered structures, such as dimers consisting of two adjacent spherical particles or "bowtie nanoantennas" comprised of two tip-to-tip triangles,[14, 16-19] which are believed to create SERS "hot spots" through strong plasmonic coupling at their junctions.[20]

The biological toxicity and chemical instability of Ag have limited the commercialization of Ag-based SERS substrates for routine application in chemical detection and medical diagnoses. Although Au represents a potential alternative, the SERS enhancements from Au nanostructures are generally significantly lower than those of similar Ag nanostructures. Additional challenges arise from the particular method used to fabricate SERS "hot spots." For instance, simple drop-casting methods based on wet chemistry yield a limited number of SERS "hot spots," since the desired dimer structures are randomly distributed, which makes the junctions between the two particles difficult to control and thereby prevents reproducible SERS measurements. Moreover, such junctions often lack mechanical stability and are subject to damage from changes in the local environment such as vibrations or temperature fluctuations. These challenges prevent the fabrication of reusable SERS substrates for routine diagnostic applications. Other commonly used methods for fabricating the "bowtie nanoantennas" heavily rely on expensive and time-consuming clean room techniques, such as e-beam lithography (EBL) or physical vapour deposition (PVD), making it costly to increase the manufacturing to achieve commercial scale. Obviously, there is a great need for developing scalable and economical processes to fabricate large-scale and robust SERS substrates that boast high sensitivity to analytes in a reproducible manner.

Herein, we report the development of a facile method to fabricate a chemically and mechanically robust SERS substrate containing well-distributed SERS "hot spots" across a large-scale polydimethylsiloxane (PDMS) elastomer through *in situ* polymerization and protonation of aniline and the subsequent

chemical reduction of Au ions. Our approach combines both soft lithography and wet chemistry methods to circumvent the tedious and costly vacuum deposition-based techniques. Aniline was chemically polymerized and protonated to form a conductive polyaniline (p-PANI, emeraldine salt) layer, which simultaneously grew on a pre-fabricated PDMS pyramid array. A conductive polymer such as polyaniline (PANI) was selected as a reducing agent of Au ions due to its π-conjugated electronic structure, which gives rise to high carrier conductivity and unique redox properties. After reducing Au^{3+} ions to form Au nanoparticles (NPs) assembled on p-PANI, the fabricated Au/p-PANI/PDMS substrates were found to exhibit substantial SERS signals with a highly reproducible EF on the order of ~10^8. Our unique approach represents a feasible way to address the current challenges limiting the development of commercially-viable SERS devices for molecular diagnostics.

Results and discussion

The fabrication process is illustrated in Fig. 1 and includes three major steps: (1) the manufacture of PDMS pyramid arrays (Fig. 1a and 1b); (2) the functionalization of the substrate surface (Fig. 1c-1e); and (3) the growth of Au NPs (Fig. 1f). The PDMS pyramid arrays were fabricated using previously reported soft-lithography techniques.[21, 22] The photolithographic method was first applied to a piece of Si (100) wafer to create square arrays of 50 × 50 μm^2. The wafer was then immersed in a 30% potassium hydroxide (KOH) solution for 25 min and then rinsed with diluted hydrogen peroxide solution (isopropanol: H_2O_2 4:1 v/v). Due to the different etching rates of Si (100) and Si (111) facets,[23] anisotropic structural arrays were constructed, as shown in Fig. 2a. The PDMS base (Sylgard 184, Dow Corning Corp.) and the curing agent were mixed in a 10:1 mass ratio and the mixture was poured onto the etched Si wafer. After polymerization, the PDMS master was peeled-off (Fig. S1) and used as a substrate for the subsequent growth of PANI and ultimately Au NP formation and assembly (Fig. 2b).

To ensure that the p-PANI fully covers the surface of the PDMS pyramid arrays, a strategy involving functionalization of the PDMS surface was employed to render it hydrophilic and facilitate the formation of a self-assembled monolayer of (3-Aminopropyl)triethoxysilane (3-APTES) as a linker for the eventual adsorption of aniline monomers.[24] The surface of the PDMS master was first functionalized with hydroxyl-terminated groups by treating with mild oxygen plasma for 5 min. The PDMS substrate was subsequently immersed in a methanol solution of 3-APTES for 24 h and dried under a gentle N_2 stream. It should be noted that the strong covalent bond between PDMS and 3-APTES is critical for the following growth of the PANI layer.[24, 25]

Due to their π-conjugated electronic structures, conductive polymers such as PANI and polypyrrole exhibit intriguing electrical properties, which give rise to high carrier conductivity and unique redox activity.[26, 27] It is believed that the polymerization of aniline monomers is an oxidative process and thus efficient polymerization is achieved in an acidic environment. In addition, it has been reported that the acids used in the synthesis of polymerization and protonation intensely impact the conductivity and stability of p-PANI films.[27-30] Here, we used ammonium peroxydisulfate (APS) and hydrochloric acid (HCl) to develop the p-PANI film. The *in situ* polymerization and deposition of a p-PANI film on a 3-APTES/PDMS substrate was carried out as follows: The substrate was first placed in an aniline/HCl solution for 20 min to adsorb the aniline molecules.[31] The substrate was then carefully washed with water to remove any remaining physisorbed aniline. Next, the substrate was covered by a mixed solution containing APS and HCl and the secondary aniline/HCl solution was added for polymerization.[31] The substrate was subsequently immersed in a 5 mM tetrachloroauric acid ($HAuCl_4$) solution until the color of the substrate surface changed from green to metallic yellow, indicating the formation of the Au film.

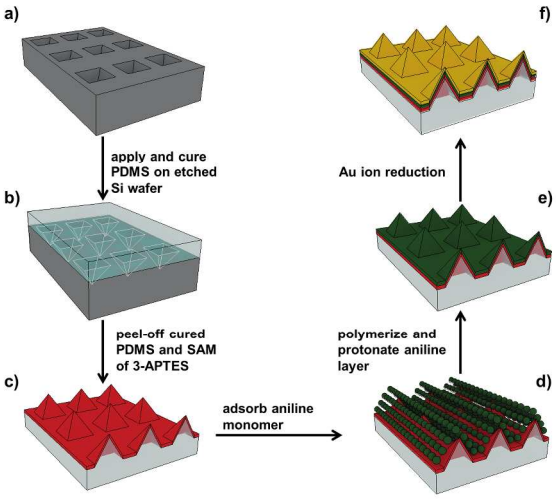

Fig. 1 A schematic diagram of the experimental procedures employed to fabricate a SERS substrate.

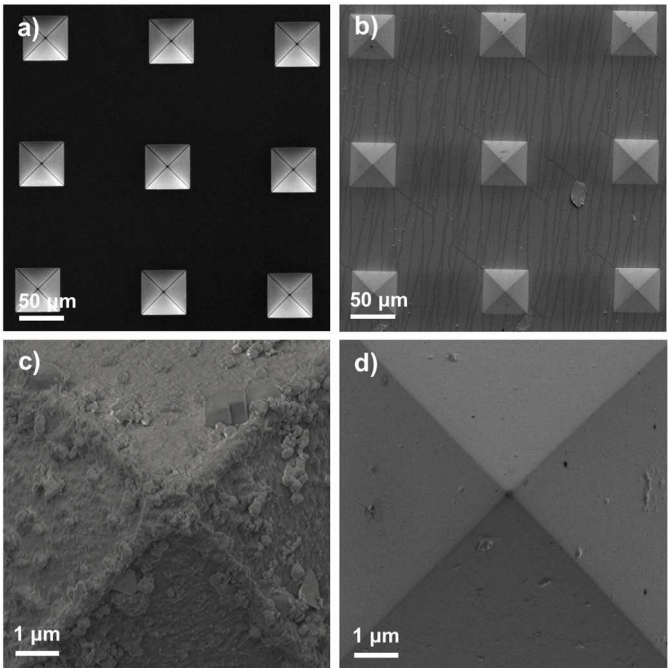

Fig. 2 SEM images demonstrating the morphology of (a) periodic inverse pyramids after the wet etch of a Si substrate; (b) fabricated pyramid arrays on PDMS with a 10 nm Au layer to facilitate imaging; (c) a Au/p-PANI/PDMS pyramid SERS substrate with rough surface features; and (d) a Au/PDMS pyramid SERS substrate fabricated using traditional e-beam evaporation.

The *in situ* growth of p-PANI generated a uniform layer on the entire surface of the PDMS substrate. It is known that the protonated PANI acts as a reducing agent for Au^{3+} reduction due to the differing reduction potentials of Au^{3+}/Au^0 and p-PANI,[32-34] yielding a conformal Au thin film on the p-PANI-covered PDMS pyramid array. Scanning electron microscopy (SEM) characterization reveals that the surface topology of the fabricated Au/p-PANI/PDMS substrate is significantly rough, and composed of aggregated Au NPs with sizes of approximately 100-250 nm (Fig. 2c). To compare our method with vacuum deposition techniques, we specifically deposited a 30 nm Au thin film directly on another PDMS pyramid array substrate via traditional electron-beam (e-beam) evaporation. As shown in Fig. 2d, the surface of such structures is much smoother and we believe the surface roughness of the Au/p-PANI/PDMS substrate plays a crucial role in enhancing Raman signals of the adsorbed molecules (*vide infra*). Further investigation of the Au/p-PANI/PDMS substrate by energy dispersive spectroscopy (EDS) and X-ray diffraction (XRD) confirms that Au NPs are formed on the p-PANI-covered pyramid array substrate (Fig. S2), and the Au NP growth is preferentially oriented along Au (111) (Fig. S3).

A commonly used Raman probe molecule, 4-aminobenzenethiol (4-ABT), was chosen to test the SERS activities of the fabricated Au/p-PANI/PDMS substrates.[35] A 785 nm laser was selected as the excitation source in order to avoid direct molecular excitation of 4-ABT during SERS measurements (Fig. S4). The blue curve in Fig. 3a shows the average Raman spectrum obtained from 30 individual Au/p-PANI/PDMS pyramids. It contains the typical enhanced vibrational signatures of 4-ABT: two major Raman features at 1079 cm^{-1} (7a, C-S stretch) and 1593 cm^{-1} (8a, C-C stretch), attributed to the enhanced EM field are easily identified in the spectrum.[36] As a comparison, the exact same SERS measurement was conducted on the Au/PDMS pyramids in which the Au thin film was deposited via e-beam evaporation (orange curve, Fig. 3a). Obviously, the Au/p-PANI/PDMS substrate shows significantly stronger SERS enhancement (detailed discussion provided in section f, ESI).

It is well known that the plasmonic "hot spots" contribute most of the Raman signals in SERS measurements, despite comprising only a modest amount of the total SERS substrate surface area.[37] To identify the topographical features of the SERS substrate responsible for the "hot spot" in an individual Au/p-PANI/PDMS pyramid, we then performed a 55×55 μm^2 Raman mapping of the SERS substrate using the 1079 cm^{-1} band. As shown in Fig. 3b, the Raman mapping includes a single Au/p-PANI/PDMS pyramid and the surrounding area. It is clear that the SERS "hot spot" is located at the tip of the pyramid with the strongest Raman signal when compared to the triangular faces of the pyramid and the surrounding flat film. Such observation is further confirmed with additional Raman mapping of four nearby Au/p-PANI/PDMS pyramids (Fig. S5, ESI). By adopting a commonly used method for the calculation of EFs (section g, ESI),[38-40] the EF of the SERS "hot spot" on the Au/p-PANI/PDMS pyramid is estimated to be ~1.4×10^8. Such a high EF (~10^8) has been suggested to be potentially sufficient for single-molecule detection.[2, 14, 15]

The large Raman enhancement observed from the Au/p-PANI/PDMS substrate comes from a combination of two major factors. As mentioned previously, the rough Au pyramid surface formed via p-PANI reduction is composed of Au NP aggregates that can induce strong plasmonic coupling between Au NPs. As seen in

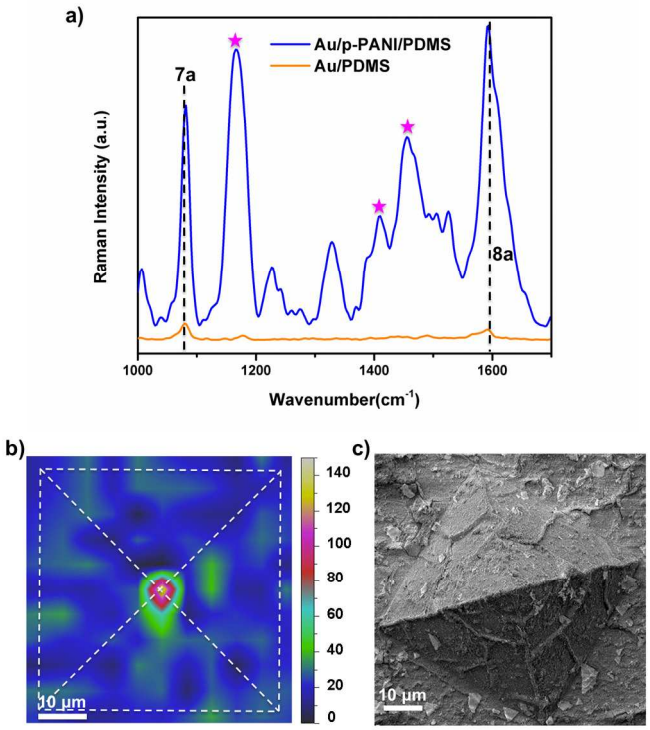

Fig. 3 SERS results obtained with 4-ABT as the Raman probe molecule. (a) comparison of SERS intensities obtained from the Au pyramid tips for the substrates fabricated via p-PANI reduction (blue) and e-beam evaporation (orange); (b) a large-area (55×55 μm^2) Raman mapping result of the 1079 cm^{-1} band acquired from a single Au pyramid (white dash line) on the p-PANI/PDMS SERS substrate, demonstrating that the strongest Raman intensity originates from the pyramid tip. The scale bar is 10 μm; (c) SEM image of the Au/p-PANI/PDMS pyramid corresponding to Raman mapping area in (b).

Fig. 2c and 2d, the Au/PDMS pyramid fabricated via e-beam evaporation shows a much smoother surface, leading to significantly lower Raman signals. Secondly, the Au tips on the Au/p-PANI/PDMS pyramids are believed to confine the SPR-enhanced EM fields and amplify the Raman signals.[41-43] It should be recognized that the surface roughness and the tip enhancement must work synergistically to produce the enormous Raman enhancement observed herein. For instance, although the triangular faces of the pyramid and the surrounding areas of the Au/p-PANI/PDMS substrates share the same surface roughness, they do not exhibit strong Raman enhancement (Fig. 3b). On the other hand, a weak Raman signal was observed on the tips of the Au/PDMS pyramids. Those observations suggest that further optimization of the Au NP size and the pyramid tip geometry will lead to additional improvements in the SERS enhancement, making our Au/p-PANI/PDMS substrates more sensitive for various chemical and biological detection schemes.

The consistent SERS enhancements from each individual Au/p-PANI/PDMS pyramid (Fig. S5, ESI) further demonstrate that our method is capable of fabricating well-distributed "hot spots" on a large scale. As mentioned previously, fabrication of SERS substrates with uniformly-distributed "hot spots" in high density remains challenging. The simple drop-casting methods only randomly produce a very limited number of SERS "hot spots" and the

commonly used EBL method heavily relies on expensive and time-consuming vacuum techniques, making it costly to scale up the manufacture of such a device. Our method combines both soft lithography and wet chemistry approaches and should be easily extendable to the fabrication of SERS platforms on a wafer scale.

The Au/p-PANI/PDMS SERS substrates are expected to be chemically and mechanically stable during extended operations. It is well known that Au is not easily oxidized and is unlikely to react with biological compounds even under harsh chemical conditions. Since the Au^{3+} ions are directly reduced on p-PANI to form Au NPs *in situ*, the p-PANI substrate functions as an adhesive to fix the positions of the Au NPs. Thus, the junctions between the two particles are secured, leading to the highly reproducible Raman signals in the SERS measurement. Additionally, such soft "glue," together with the flexible PDMS template, ensures that the fabricated Au/p-PANI/PDMS SERS substrates exhibit substantial mechanical stability. Fig. S6 shows the Raman mapping of the exact same Au/p-PANI/PDMS pyramid shown in Fig. 3b after bending the SERS substrate thirty times three months after the initial measurement. Under the same experimental conditions, the pyramid tips still exhibit strong Raman enhancement with intensities similar to the initial measurement.

Conclusions

In conclusion, the thoughtful combination of soft lithography and wet chemistry techniques has enabled the fabrication of chemically robust and mechanically flexible SERS substrates. The prepared substrates exhibit significantly strong SERS signals to facilitate molecular detection, boasting large SERS EFs of ~10^8 orders of magnitude. More importantly, the engineered "hot spots" are uniformly distributed in a large-scale area with consistent SERS enhancements. Since there is no requirement for costly clean-room techniques, our simple and cost-effective method offers the potential opportunity for the fabrication of commercially-viable SERS substrates applicable to Raman-based molecular diagnostics.

Experimental section

Materials

Aniline (99.5%, extra pure), ammonium peroxydisulfate (APS), (3-Aminopropyl)triethoxysilane (3-APTES), and tetrachloroauric acid trihydrate ($HAuCl_4 \bullet 3H_2O$) were purchased from Sigma Aldrich. Polydimethylsiloxane (PDMS) and its curing agent were obtained from Dow Corning Corporation, Inc. Shipley 1813 photoresist was bought from MicroChem. Hydrochloric acid (HCl) and potassium hydroxide (KOH) were purchased from Fisher Scientific.

Synthesis and SERS substrate preparation

The creation of inverse pyramid arrays on a Si wafer and the fabrication of PDMS pyramid arrays were in accordance with previous reports.[21, 22] A patterned PDMS substrate was exposed to oxygen plasma for 5 min before being immersed in a 5 mM of 3-APTES solution for 24 h. The substrate was then carefully washed with methanol and water and dried using a mild N_2 stream. Subsequently, the substrate was dipped in an aniline/HCl solution (0.17 g of aniline in 26 mL of 1.0 M HCl) for 20 min to adsorb aniline molecules, as described elsewhere.[31] Then, the substrate was rinsed with water to remove the physisorbed aniline molecules and placed into a Pyrex beaker. The polymerization solution containing APS/HCl (0.14 g of APS in 10 mL of 1.0 M HCl) and the growth solution of aniline/HCl (0.06 g aniline in 26 mL of 1.0 M HCl) were sequentially added to the beaker. After 30 min, the substrate turned light green. In order to make sure the protonated polyaniline (p-PANI) formed a well-covered film on the PDMS substrate, we removed the substrate after 12 h. Finally, we immersed the dried p-PANI/PDMS substrate into a 5 mM $HAuCl_4$ aqueous solution for 3 h. The Au/p-PANI/PDMS substrate was immersed in a 1×10^{-3} M 4-ABT solution in methanol overnight and was washed with methanol to remove the physisorbed molecules.

Characterization

The morphology of the sample was characterized using scanning electron microscopy with an acceleration voltage of 5 kV (Nova NanoSEM, FEI). The elemental analysis was carried out using energy dispersive spectroscopy (EDS) equipped with the SEM. The collection was performed under 20000x magnification using an acceleration voltage of 10 kV. X-ray diffraction (XRD) patterns were obtained using an X'Pert powder diffractometer (PANalytical Systems) with Cu Kα radiation (λ = 1.5406 Å). The extinction spectra were measured using a Zeiss Observer Zm.1 inverted microscope equipped with a Craic QDI 302™ spectrophotometer. The SERS measurements were conducted with a Horiba LabRAM microRaman using a 785 nm diode laser focused with a 50x objective lens. The laser spot size is ~2 μm and the incident power used in our measurements was ~0.1 mW. The acquisition time was set for 5 s for tip measurements and was set for 10 s for measurements on the Au flat film deposited by e-beam evaporation. For a Raman image with a scanning range of 55×55 μm^2, the integration time was 0.2 s per spectrum with a step size of 0.7 μm. All Raman images were converted by integrating the intensity of Raman signal at 1079 cm^{-1}, which is ascribed to the vibration of C-C stretch of 4-ABT.[36]

Acknowledgements

This work is supported by NSF under grant CHE-1308644, and partially by CHE-1038015, the CCI Center for Nanostructured Electronic Materials. W.D.W. acknowledges support from ORAU for the Ralph E. Powe Junior Faculty Enhancement Award, Sigma Xi for the Junior Faculty Research Award from the Florida Chapter and the University of Florida (UF) for startup assistance. Materials characterization was conducted at the Nanoscale Research Facility (NRF) and the Major Analytical Instrumentation Center (MAIC) at UF. The authors also thank Tzu-Yin Wang and Yu-Ting Chang for artwork.

Notes and references

[a]*Department of Chemistry and Center for Nanostructured Electronic Materials, University of Florida, Gainesville, FL 32611, USA*
**Fax: +1-352-392-0872; Tel: +1-352-392-2050;*

E-mail: wei@chem.ufl.edu
[b]*Jiangsu-Singapore Joint Research Center for Organic/Bio- Electronics & Information Displays and Institute of Advanced Materials (IAM), Nanjing Tech University, 30 South Puzhu Road, Nanjing 211816, China*
†Electronic Supplementary Information (ESI) available: Digital image of the PDMS substrate, the EDS , XRD, and optical extinction data of the Au/p-PANI/PDMS substrate, additional Raman mapping images, discussion of SERS spectrum, and the calculation of SERS enhancement factor. See DOI: 10.1039/c000000x/

1. K. A. Willets and R. P. Van Duyne, *Annu. Rev. Phys. Chem.*, 2007, **58**, 267-297.
2. E. C. Le Ru and P. G. Etchegoin, in *Annual Review of Physical Chemistry,* ed. M. A. Johnson and T. J. Martinez, Annual Reviews, Palo Alto, 2012, vol. 63, pp. 65-87.
3. Y. W. C. Cao, R. C. Jin and C. A. Mirkin, *Science*, 2002, **297**, 1536-1540.
4. Y. C. Cao, R. C. Jin, J. M. Nam, C. S. Thaxton and C. A. Mirkin, *J. Am. Chem. Soc.*, 2003, **125**, 14676-14677.
5. X. Huang, I. H. El-Sayed, W. Qian and M. A. El-Sayed, *Nano Lett.*, 2007, **7**, 1591-1597.
6. S. J. Tan, M. J. Campolongo, D. Luo and W. L. Cheng, *Nat. Nanotechnol.*, 2011, **6**, 268-276.
7. G. Schatz, M. Young and R. Duyne, in *Surface-Enhanced Raman Scattering*, ed. K. Kneipp, M. Moskovits and H. Kneipp, Springer Berlin Heidelberg, 2006, vol. 103, ch. 2, pp. 19-45.
8. K. Kneipp, Y. Wang, H. Kneipp, L. T. Perelman, I. Itzkan, R. Dasari and M. S. Feld, *Phys. Rev. Lett.*, 1997, **78**, 1667-1670.
9. W. Wei, S. Li, J. E. Millstone, M. J. Banholzer, X. Chen, X. Xu, G. C. Schatz and C. A. Mirkin, *Angew. Chem. Int. Ed.*, 2009, **48**, 4210-4212.
10. M. J. Banholzer, J. E. Millstone, L. Qin and C. A. Mirkin, *Chem. Soc. Rev.*, 2008, **37**, 885-897.
11. R. Bukasov, T. A. Ali, P. Nordlander and J. S. Shumaker-Parry, *ACS Nano*, 2010, **4**, 6639-6650.
12. S. M. Ansar, X. Li, S. Zou and D. Zhang, *J. Phys. Chem. Lett.*, 2012, **3**, 560-565.
13. Z. Zhu, H. Meng, W. Liu, X. Liu, J. Gong, X. Qiu, L. Jiang, D. Wang and Z. Tang, *Angew. Chem. Int. Ed.*, 2011, **50**, 1593-1596.
14. J. P. Camden, J. A. Dieringer, Y. M. Wang, D. J. Masiello, L. D. Marks, G. C. Schatz and R. P. Van Duyne, *J. Am. Chem. Soc.*, 2008, **130**, 12616-12617.
15. W.-H. Park and Z. H. Kim, *Nano Lett.*, 2010, **10**, 4040-4048.
16. S. Dodson, M. Haggui, R. Bachelot, J. Plain, S. Li and Q. Xiong, *J. Phys. Chem. Lett.*, 2013, **4**, 496-501.
17. Z. H. Zhu, T. Zhu and Z. F. Liu, *Nanotechnology*, 2004, **15**, 357-364.
18. J. Theiss, P. Pavaskar, P. M. Echternach, R. E. Muller and S. B. Cronin, *Nano Lett.*, 2010, **10**, 2749-2754.
19. D. Wang, W. Zhu, M. D. Best, J. P. Camden and K. B. Crozier, *Nano Lett.*, 2013, **13**, 2194-2198.
20. G. Lu, H. Li, S. Wu, P. Chen and H. Zhang, *Nanoscale*, 2012, **4**, 860-863.
21. F. W. Huo, G. F. Zheng, X. Liao, L. R. Giam, J. A. Chai, X. D. Chen, W. Y. Shim and C. A. Mirkin, *Nat. Nanotechnol.*, 2010, **5**, 637-640.
22. D. Qin, Y. N. Xia and G. M. Whitesides, *Nat. Protoc.*, 2010, **5**, 491-502.
23. I. Zubel and M. Kramkowska, *Sensors Actuat. A-Phys.*, 2004, **115**, 549-556.
24. S. S. Patil, S. P. Koiry, P. Veerender, D. K. Aswal, S. K. Gupta, D. S. Joag and M. A. More, *RSC Adv.*, 2012, **2**, 5822-5827.
25. V. Sunkara, D. K. Park, H. Hwang, R. Chantiwas, S. A. Soper and Y. K. Cho, *Lab Chip*, 2011, **11**, 962-965.
26. J. Stejskal and R. G. Gilbert, *Pure Appl. Chem.*, 2002, **74**, 857-867.
27. N. Gospodinova and L. Terlemezyan, *Prog. Polym. Sci.*, 1998, **23**, 1443-1484.
28. M. Vecino, I. González, M. E. Muñoz, A. Santamaría and J. A. Pomposo, *Polymer*, 2003, **44**, 5057-5059.
29. D. W. Hatchett, M. Josowicz and J. Janata, *J. Phys. Chem. B*, 1999, **103**, 10992-10998.
30. A. Pud, N. Ogurtsov, A. Korzhenko and G. Shapoval, *Prog. Polym. Sci.*, 2003, **28**, 1701-1753.
31. C.-H. Chiang and C.-G. Wu, *Chem. Commun.*, 2010, **46**, 2763-2765.
32. P. Xu, N. H. Mack, S.-H. Jeon, S. K. Doorn, X. Han and H.-L. Wang, *Langmuir*, 2010, **26**, 8882-8886.
33. P. Xu, S.-H. Jeon, H.-T. Chen, H. Luo, G. Zou, Q. Jia, M. Anghel, C. Teuscher, D. J. Williams, B. Zhang, X. Han and H.-L. Wang, *J. Phys. Chem. C*, 2010, **114**, 22147-22154.
34. S. W. Li, P. Xu, Z. Q. Ren, B. Zhang, Y. C. Du, X. J. Han, N. H. Mack and H. L. Wang, *ACS Appl. Mater. Interfaces*, 2013, **5**, 49-54.
35. P. Fenter, A. Eberhardt and P. Eisenberger, *Science*, 1994, **266**, 1216-1218.
36. K. Kim and H. S. Lee, *J. Phys. Chem. B*, 2005, **109**, 18929-18934.
37. Y. Fang, N.-H. Seong and D. D. Dlott, *Science*, 2008, **321**, 388-392.
38. Q. Yu, P. Guan, D. Qin, G. Golden and P. M. Wallace, *Nano Lett.*, 2008, **8**, 1923-1928.
39. Z.-Q. Tian, B. Ren and D.-Y. Wu, *J. Phys. Chem. B*, 2002, **106**, 9463-9483.
40. K. Kim, D. Shin, H. B. Lee and K. S. Shin, *Chem. Commun.*, 2011, **47**, 2020-2022.
41. J. F. Li, Y. F. Huang, Y. Ding, Z. L. Yang, S. B. Li, X. S. Zhou, F. R. Fan, W. Zhang, Z. Y. Zhou, Y. WuDe, B. Ren, Z. L. Wang and Z. Q. Tian, *Nature*, 2010, **464**, 392-395.
42. R. M. Stockle, Y. D. Suh, V. Deckert and R. Zenobi, *Chem. Phys. Lett.*, 2000, **318**, 131-136.
43. B. Pettinger, B. Ren, G. Picardi, R. Schuster and G. Ertl, *Phys. Rev. Lett.*, 2004, **92**, 096101.